TECTONICS, VOL. 7, NO. 5, PAGES 975-989, OCTOBER 1988

SEISMOGENIC STRIKE-SLIP FAULTING AND THE DEVELOPMENT OF THE NORTH CHINA BASIN

Wang-Ping Chen

Department of Geology, University of Illinois, Urbana

John Nábelek

College of Oceanography, Oregon State University, Corvallis

Abstract. The actively subsiding North China sedimentary basin is associated with an unusually high level of seismic activity. This oil- and gas-producing basin has been the site of nine large ($M \geq 7$), destructive earthquakes since 1600 A. D. An analysis of faulting during the Tangshan earthquake sequence, which includes some of the largest shocks that have occurred in this basin during the past 400 years, showed that the dominant pattern of deformation during this sequence was associated with displacement on right-stepping, right-lateral strike-slip faults. A large amount of subsidence (~1.0–1.5 m) occurred in pull-apart regions between steps of the north-northeast (NNE) trending strike-slip faults. The directivity of the P wave radiation pattern and the distribution of aftershocks of the Bohai Gulf earthquake of July 18, 1969, also indicate strike-slip faulting on planes of similar NNE trend. Together with the four largest shocks of the Hsingtai sequence in 1966, earthquakes with right-lateral slip on NNE trending faults account for about two-thirds of the seismic moment released in this region for the past 100 years. The average regional strain due to seismic slip has a dominant component of dextral simple shear (on NNE striking planes) that is approximately twice as large as north-south extension or east-west shortening. Based on a combination of published field and borehole data, the dominance of horizontal dextral simple shear over subsidence seems to have begun no later than the mid-Pliocene and the total amount of extension over the entire basin is only about 20–30%. This pattern of deformation, the spatially variable heat flow values, the scattered locations of rapid deposition of Quaternary sediments, and the fluctuating rate of sedimentation in space and time during the Neogene in this basin are difficult to explain by pure extension and thermal subsidence. We propose that these observations, and the shape of the whole North China basin (that of a "lazy Z"), are a consequence of pulling-apart associated with right-lateral movement on the NNE trending strike-slip fault systems and that the basin as a whole has formed and evolved as a composite pull-apart basin due to right-lateral slip on numerous right-stepping faults since the Eocene.

Paper number 8T0341.
0278–7407/88/008T–0341$10.00

INTRODUCTION

The North China basin is a large (~2×10^5 km^2) intracratonic sedimentary basin (Figure 1) producing oil and gas [e.g., Li, 1981]. The basement of the basin has a long geologic history, but the most recent phase of major tectonic activity started in the Eocene [Lee, 1986; Li, 1982]. The post-Eocene history of subsidence in the basin has been qualitatively explained by a two-stage evolutionary model that has been commonly applied to intracontinental basins [McKenzie, 1978]: A basin is formed by a brief initial period of fault controlled rifting, followed by long-term gradual thermal subsidence. According to this model, the thermal subsidence stage in the North China basin began in the Neogene and is continuing today [Ye et al., 1985]. A recent analysis by Hellinger et al. [1985], however, demonstrates that the history of subsidence in this basin cannot be modeled by either a one-layer model of crustal extension, or a two-layer model of continental stretching [Hellinger and Sclater, 1983]. Therefore alternative tectonic models must be examined.

Unlike many other oil-producing basins, the North China basin has an extremely high level of seismic activity. Nine earthquakes with magnitudes (M) greater than or equal to 7 have occurred within the basin since 1600 A. D. (Figure 1). Many of these large shocks were accompanied by foreshock-aftershock activity, containing events as large as $M \geq 6$

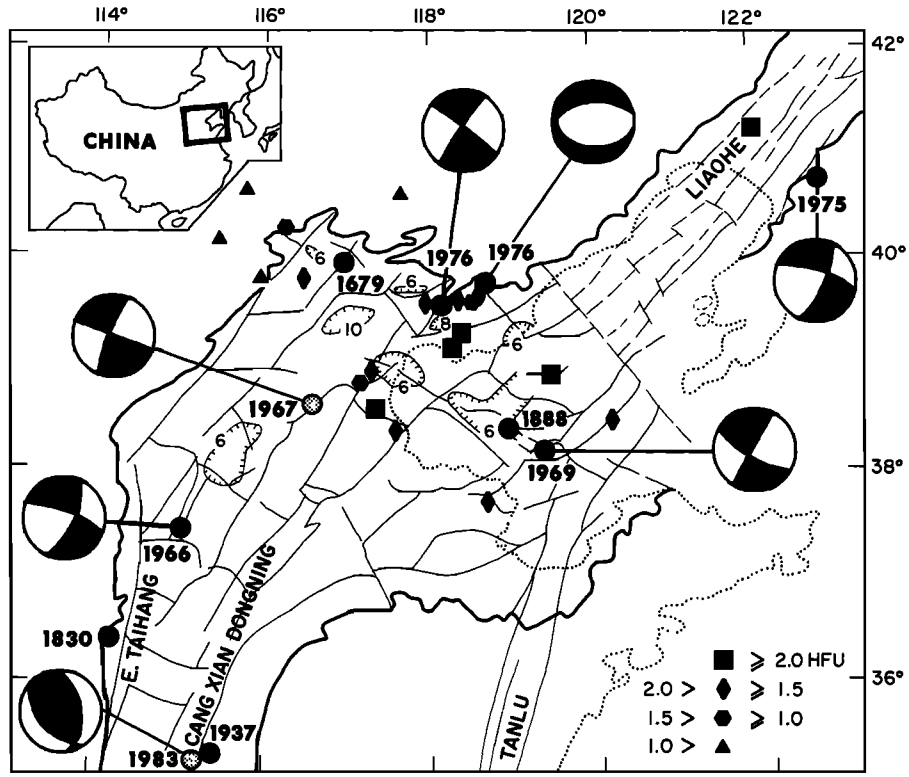

Fig.1. Map of the North China basin summarizing recent and historical seismicity, heat flow, structure, and sedimentation since the Quaternary. The present boundary of the basin is shown by thick solid lines, known faults by thinner solid lines (dashed when less certain), and coastline by dotted curves. Depocenters of Quaternary sediments are shown as depressions with isopachs (in 100 m) marked. Solid circles are epicentral regions of large ($M > 7$) earthquakes and earthquake sequences since 1600 A. D. (modified from Figures 10 and 12 of Ye et al. [1985]). Shaded circles are epicenters of earthquakes with $6 < M < 7$ since 1964. The location of a thrust event on November 6, 1983 (M_o~2.4 x 10^{17} Nm; Dziewonski et al. [1984]) is also plotted. The "beach ball" symbols show lower hemisphere, equal area projections of the centroidal nodal plane solutions of earthquakes (Table 1) with the compressional quadrants darkened. Sites of measured surface heat flow (taken from Ye et al. [1985]) are marked: squares for ≥ 2.0 HFU (HFU = μcal/cm²s = 42 mW/m²), diamonds for 1.5–2.0 HFU, hexagons for 1.0–1.5 HFU, and triangles for < 1.0 HFU. Notice that high values (> 100 mW/m²) occur next to low values (~50 mW/m²) and that the depocenters of Quaternary sediments are not interconnected.

(Table 1). Since the installation of the World-Wide Standard Seismograph Network (WWSSN) in 1964, the fault plane solutions and aftershock distribution for the largest earthquakes in this region indicate right-lateral strike-slip faulting on north-northeast (NNE) trending planes (Figure 1). The only large event with normal faulting mechanism is the largest aftershock of the Tangshan sequence (July 28, 1976). Thus faulting has continued in this basin long after the presumed initial stage of pre-Neogene crustal thinning. More importantly, the pattern of present-day faulting reflected by earthquake data seems to show a predominance of strike-slip motion over subsidence.

In this study we present results of an analysis of teleseismic body waves for the Bohai Gulf event of 1969, and we review faulting associated with the Tangshan earthquake sequence of 1976, as well as that of two other major events which occurred in this basin since 1966. We further synthesize the results from seismic observations recorded at both teleseismic and local distances, field and macroseismic observations, and geodetic data. Our results show that right-lateral slip on faults trending approximately NNE is the dominant mode of deformation during the largest earthquake sequences. Consequently, the same pattern is observed in the regional strain due to seismicity. We also discuss other observations in the North China basin which cannot be explained easily by pure crustal-stretching models of basin formation, and we develop an alternative interpretation that the basin as a whole can be viewed as a large composite pull-apart system.

DEFORMATION ASSOCIATED WITH MAJOR EARTHQUAKE SEQUENCES

Tangshan Earthquake Sequence

On a scale of 10–100 km, earthquake faulting and its relationship to local subsidence of the North China basin is

TABLE 1. A Summary of Recent and Historical (since 1600) Seismicity of the North China Basin

Number	Date	Latitude, °N	Longitude, °E	Origin Time, hr:min:s	M_s or M	m_b or M_l	References	M_o, Nm	Focal Depth, km	Strike, Dip, Rake, degrees	References
				1600–1900 A. D., $M \geq 7$							
1	Sept. 2, 1679	40.0	117.0		8.0		1				
2	June 12, 1830	36.4	114.2		7.5		1				
3	June 13, 1888	38.5	119.0		7.5		1				
				Heze							
4	Aug. 1, 1937	35.3	115.4	10:41:05	7.0^3		2				
		(35.2)	(115.3)	(10:41:03)			4				
				Tangshan							
5	Sept. 23, 1945	39.7	118.7	15:34:23	6.3		2				
		(40.1)	(118.8)				4				
				Hsingtai							
6	March 7, 1966	37.35	114.92	21:29:14	6.8	5.6	5	1.0×10^{19}	11	208,89,182	5
7	March 22, 1966	37.50	115.08	08:11:36	6.7	5.6	5	3.0×10^{18}	8	208,82,182	5
8	March 22, 1966	37.53	115.05	08:19:46	7.2	5.9	5	1.8×10^{19}	9	26,73,191	5
9	March 26, 1966	37.68	115.27	15:19:04	6.2	5.2	5	1.4×10^{18}	9	30,74,203	5
10	March 29, 1966	37.47	114.88	06:11:59	6.		2				
				Hejian							
11	March 27, 1967	38.56	116.61	08:58:20	6.3		3			(202,80,177)	6
				Bohai							
12	July 18, 1969	38.43	119.47	05:24:49	7.4^2		3				
				Subevent 1				4.0×10^{19}	6	209,87,200	This
				Subevent 2				2.1×10^{19}	9	356,80,183	Study
				Haicheng							
13	Feb. 4, 1975	40.65	122.80	$11:36:08^8$	7.3	6.4^8	3	3.0×10^{19}	10	288,78,342	8
20	May 18, 1978	40.71	122.61	$12:33:31^{10}$	6.0		9		7	(106,84,-20)	10
				Tangshan							
14	July 27, 1976	39.63	118.18	19:42:56	7.8^3	6.1^4	11				
				Subevent 1				3.5×10^{19}	12	185,78,183	7
				Subevent 2				5.8×10^{19}	7	225,80,157	7
				Subevent 3				2.7×10^{19}	15	(95,41,111)	7
15	July 28, 1976	39.67	118.57	10:45:37	7.1^3	6.1^4	12	3.0×10^{19}	8	(260,50,261)	7
16	Nov. 15, 1976	39.44	117.83	13:53:01	6.8^4	6.0^4	13	2.6×10^{18}	18	322,67,350	7
17	Aug. 31, 1976	39.91	118.90	03:25:01	5.3	5.2	4	1.6×10^{17}	6	(253,67,217)	7
18	March 7, 1977	40.10	117.74	00:28:48	5.0	5.2	4	1.2×10^{17}	7	(220,65,221)	7
19	May 12, 1977	39.28	117.84	11:17:54	5.9^4	5.6^4	13	3.8×10^{17}	16	311,69,2	7
21	Oct. 19, 1982	39.95	119.01	20:45:59		5.3	14				
				Heze							
22	Nov. 6, 1983	35.21	115.17	21:09:51			15	2.4×10^{17}	(21)	(142,44,71)	15

Event numbers are in chronological order. Orientation of only one of the nodal planes is given in parentheses for those events whose true fault planes are unknown. All events whose seismic moments are known have been included in expression (5). References: 1, Seismological Committee of the Academia Sinica [1956]; 2, Lee et al. [1978]; 3, Molnar and Deng [1984]; 4, International Seismological Summary or Bulletin of the International Seismological Center; 5, Chung and Cipar [1983]; 6, Tapponnier and Molnar [1977]; 7, Nábelek et al. [1987]; 8, Cipar [1979]; 9, Xiang et al. [1980]; 10, Shedlock et al. [1985]; 11, State Seismological Bureau [1982]; 12, Zhang et al. [1980]; 13, Shedlock et al. [1987]; 14, Peng et al. [1985]; 15, Dziewonski et al. [1984].

best illustrated by deformation associated with the Tangshan earthquake sequence of 1976. Nábelek et al. [1987] have performed a detailed analysis of P and SH waves generated by the six strongest shocks of this sequence. They also gave a detailed discussion of several other seismic studies of this sequence [e.g., Butler et al., 1979; Kikuchi and Kanamori, 1986]. In this section we shall briefly summarize the deformation of the entire sequence.

The main shock was associated with right-lateral slip on a nearly vertical fault trending approximately N30°E over a length of about 100 km (the Tangshan fault, segments A and B in Figure 2). The detailed history of rupture of the main shock is complex, including a change in the strike of the fault from north-northeast to northeast (Figure 2) and thrust faulting which took place south of the epicenter during the last phase of the rupture [Nábelek et al., 1987]. Nevertheless, the

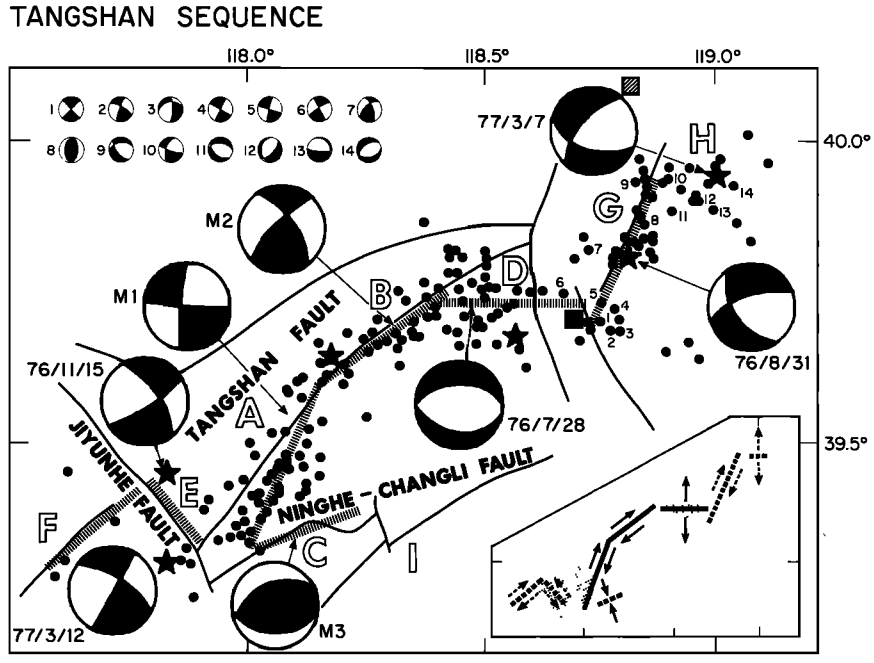

Fig. 2. A detailed map of faulting during the Tangshan earthquake sequence (taken from Nábelek et al. [1987]). Mapped geological faults (solid lines) in the area are plotted together with the epicenters of 200 aftershocks (circles) located by Shedlock et al. [1987]. For simplicity, not all known faults are plotted. Heavy dashed lines are our interpretation of the gross shape of fault segments that were activated during the Tangshan sequence (Table 1). The epicenters of the six largest events (stars) [State Seismological Bureau, 1982; Shedlock et al., 1987] and the large event in 1945 reported by the International Seismological Summary (1945) (shaded square) are shown. The location of the last event based on macroseismic data and reported in the catalogue of Lee et al. [1978] is shown by a solid square. Also plotted are the fault plane solutions of the three subevents of the main shock (M1, M2, and M3) and the five largest aftershocks determined by Nábelek et al. [1987]. Fault plane solutions for the numbered events in the northeastern portion of the aftershock zone determined by Shedlock et al. [1987] from first motions are shown in the upper left corner of the figure. In the insert the arrows near each segment indicate the inferred direction of relative displacement (dashed when less certain). Regions of subsidence (up to 1.5 m) [Zhang et al., 1981] are observed near segments D and E where the main right-lateral fault system steps toward the right (pull-apart). The shaded areas outline the regions where subsidence is > 0.5 m.

predominant mode of slip along the north-northeast trending Tangshan fault is right-lateral as evidenced from earthquake mechanisms [Nábelek et al., 1987], geodetic measurements [Zhang et al., 1981], and surface ruptures [Guo et al., 1977].

Fifteen hours after the main shock, a large aftershock (the Luanxian earthquake) occurred to the northeast of the main shock on a fault marked as segment D in Figure 2. The mechanism of this shock is tightly constrained as normal faulting on an east-west trending plane [Nábelek et al., 1987]. This segment is also delineated by about 10 events ($4 \leq M_l \leq 5$) which occurred between July 1982 and March 1983 [Peng et al., 1985]. A detailed location of some 200 aftershocks which occurred as late as December 1979 [Shedlock et al., 1987] placed about a dozen epicenters to the east of segment D extending to near 119°E (Figure 2). Shedlock et al. [1987] connected these events with those near the junction of segments B and D (Figure 2), and they postulated a west-northwest trending strike-slip segment extending from about 118.5° to 119°E. While the existence of such a segment is subject to interpretation, we note that the moment release of the Luanxian earthquake is at least two orders of magnitude greater than the combined moment of all the small aftershocks in that region. This, together with the analysis of geodetic leveling data obtained before (in 1975) and 6 months after the Tangshan sequence [Zhang et al., 1981], which showed relative subsidence of up to 1.0 m (Figure 2), leads us to interpret segment D as a major pull-apart feature where the right-lateral Tangshan fault steps toward the right.

There is no direct evidence for a large amount of slip on segment G during the Tangshan sequence, although many aftershocks occurred there. Two largest aftershocks there show a mixture of strike-slip and normal faulting (Figure 2). The fault plane solutions of small aftershocks at the southern end of G also show largely strike-slip faulting (events 1–6, Figure 2). The distribution of aftershocks is irregular but an overall NNE trend can be identified (Figure 2). At the northern end of

G the seismicity becomes deeper and is again characterized by normal faulting [Shedlock et al., 1987]. It is conceivable that the northern end of G marks another pull-apart region (H in Figure 2).

Characteristics of pull-apart related to right-stepping of right-lateral faults are also apparent at the southern end of the Tangshan fault. Two large aftershocks occurred near the intersection of the Tangshan and the Jiyunhe fault (Figure 2; segment E). Both aftershocks involved either left-lateral slip on the conjugate fault E, or right-lateral slip on F and/or A. Field observations suggest that left-lateral slip took place along fault segment E [Li and Guo, 1979]. Either way, a substantial amount of extension must have occurred between segments A and F near E, as is evident from the releveling data. The maximum subsidence here reached 1.5 m [Zhang et al., 1981], which is of the same order as that observed at segment D.

Approximately 20 s after the onset of the main shock, a subevent with a large component of thrust faulting occurred south of the epicenter near segment C (Figure 2). The occurrence of thrust faulting in an actively subsiding basin appears surprising at first glance. However, we note that local uplift is known to occur in pull-apart basins that have developed in association with major strike-slip faults where the strike-slip (master) fault changes direction slightly [e.g., Crowell, 1974; Freund, 1971]. Alternatively, local compression can occur at left-steps of subparallel right-lateral faults [e.g., Segall and Pollard, 1980; Sharp, 1972]. Both mechanisms are possible during the Tangshan sequence [Nábelek et al., 1987], and they are expressions of transpression in a strike-slip regime [Harland, 1971; Sanderson and Marchini, 1984]. It is also possible that local compression can result from block rotation in a system of parallel strike-slip faults [e.g., Nur et al., 1986]. In any case, it is important to note that the effect of local compression is overwhelmed by that of pull-apart in the overall static deformation during the Tangshan sequence because releveling data showed only net subsidence reaching a maximum of over 1 m [Zhang et al., 1981].

Elsewhere in the basin, a moderate-sized event (November 6, 1983; M_o~2.4×10^{17} Nm) occurred on the southern edge of the basin near the epicenter of the large (M = 7) event in 1937 (Figure 1 and Table 1). The preliminary result of Dziewonski et al. [1984] shows pure thrust faulting. The P axis of this event is consistent with those of the strike-slip events, indicating a regional compression along east-northeast (ENE) (Figure 1). Tapponnier and Molnar [1976, 1977] interpreted the regional stress field near the North China basin as a result of the continental collision between India and Eurasia. Although the exact cause of the thrust faulting event is not known, its occurrence is generally consistent with this regional compression. In contrast, simple crustal thinning models cannot easily account for the occurrence of thrust faulting.

Other Major Earthquakes

On a basin-wide scale the northeast (NE) to NNE trending fractures seem to be the dominant structural trend throughout the basin (Figure 1). In addition to the Tangshan sequence, right-lateral strike-slip motion on NE to NNE trending planes was associated with two other large earthquake sequences.

Bohai Gulf. The seismic moment release (~6×10^{19} Nm) of the Bohai Gulf event of 1969 is exceeded only by that of the main shock of the Tangshan sequence. The Bohai Gulf event occurred offshore and the only available data are teleseismic recordings and locations of epicenters of the larger aftershocks by a regional seismic network in northeastern China.

Following the inversion procedure outlined by Nábelek [1984], we have determined the seismic moment, the orientation of the nodal planes, and the depth of this event (Figure 3 and Table 2) by formally inverting the waveforms and amplitudes of 16 teleseismic ($30° \leq \Delta \leq 90°$) P waves recorded by the long-period instruments of the WWSSN. The recordings of S waves went off-scale and could not be analyzed. Details of the data processing and the assumptions on velocity structure and attenuation are the same as those for the Tangshan sequence [Nábelek et al., 1987] whose source-receiver configuration is nearly identical to that of the Bohai sequence.

For this event all the seismograms have high signal-to-noise ratios and cover a wide azimuthal range. The mechanism of predominantly strike-slip faulting (Figure 3) is well constrained. The source time function of about 40-s duration shows two bursts of moment release: one at the onset of the signal and the other about 20 s later (Figure 3), indicating the existence of at least two subevents. The two subevents are sufficiently separated in time that a slight change in the orientation of their nodal planes can be resolved (Figure 3a).

In order to differentiate the fault plane from the auxiliary nodal plane, we carried out analyses with the rupture propagating in each of the four possible directions up and down the strikes of both nodal planes for the first subevent, which accounts for two-thirds of the total moment release. We found that a propagating rupture from south to north along the NNE trending nodal plane is required for the first subevent in order to match the overall distribution of amplitudes and the strong initial swing observed at stations to the northeast of the epicenter (e.g., COL, LON, and BKS; Figure 3a). For comparison, Figure 3b shows the next best solution of a eastward propagating rupture. Such a solution clearly provides a poorer overall match than a northward propagating source and cannot reproduce the large amplitudes observed to the north of the epicenter. Thus the directivity of the P waves strongly suggests that the main shock was associated with right-lateral slip on the NNE trending plane. The data also indicate that the second subevent occurred approximately 15 km to the northwest of the first but its exact relative position cannot be resolved.

The aftershocks of the Bohai earthquake formed a band trending approximately NNE and they again suggest that the fault plane strikes in that direction (Figure 4). The quality of the location of the aftershocks is probably marginal. Nonetheless, the trend in the NNE direction is clear and its length (about 50 km) is at least twice the dimension of its width. Since the overall shape of the distribution of aftershocks of the Tangshan sequences determined by routine locations [Tangshan Seismological Team, 1981] does not differ significantly from that of more elaborate locations [Shedlock et al., 1987] in the same region, this NNE trend is

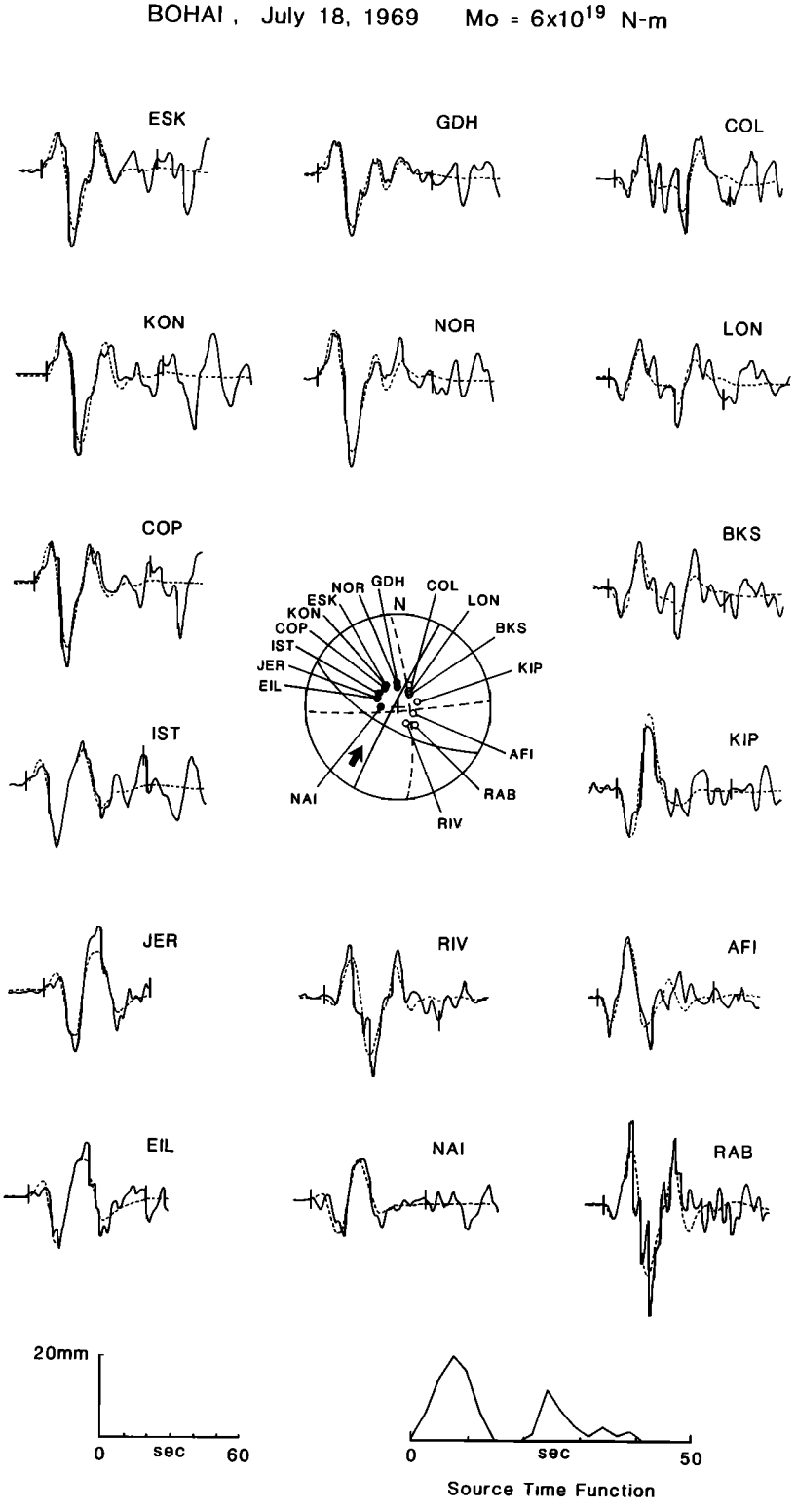
BOHAI , July 18, 1969 Mo = 6x10^19 N-m
ESK
GDH
COL
KON
NOR
LON
COP
BKS
IST
KIP
JER
RIV
AFI
EIL
NAI
RAB
N
20mm
0
sec
60
0
sec
50
Source Time Function

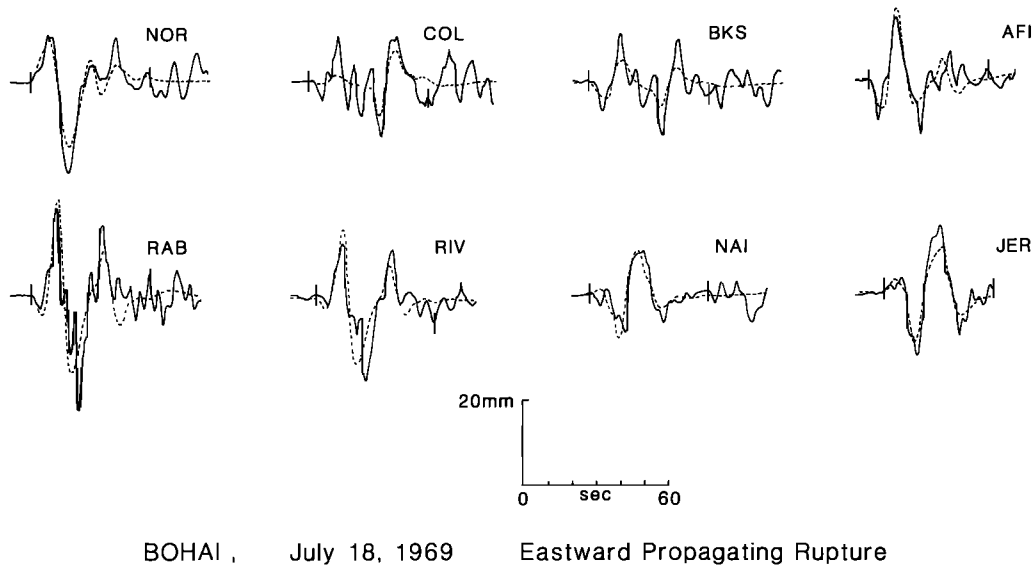

Fig. 3b. The observed and synthetic seismograms generated for a model with an eastward propagating rupture. The stations shown are the ones most sensitive to the assumed direction of rupture. This model fails to reproduce the observed amplitudes at stations to the north of the epicenter (e.g., COL, BKS, and NOR), even though a slightly better fit is found at RAB to the east of the epicenter. Models with other directions of propagation (including no rupture propagation) were tested, but they do not match the observations in most azimuths.

unlikely to be a consequence of systematic errors in locations. We conclude that the Bohai Gulf event is primarily associated with right-lateral slip on the nodal plane striking NNE.

Hsingtai (Xingtai). The Hsingtai earthquake swarm of 1966 produced no surface breaks. However, the locations of the largest shocks, as well as the distribution of aftershocks suggest that they occurred on a sequence of NNE trending right-lateral faults along edges of a graben [e.g., Chung and Cipar, 1983]. The sum of the scalar seismic moments for the three largest shocks of the Hsingtai swarm is about 3.2×10^{19} Nm, or approximately half of the moment of the Bohai Gulf earthquake.

Haicheng. The only other large event whose seismic moment can be determined is the famous Haicheng earthquake of 1975. Because of numerous foreshocks its occurrence was successfully predicted. Relocation of aftershocks defines a scattered band of activity trending west-northwest (WNW) [Shedlock et al., 1985], suggesting that this is the orientation of the fault plane. Although no surface rupture has been found for this earthquake, some field information is available from a sparse geodetic network surveyed in 1958 and then again in 1975 after the main shock [Wu et al., 1976].

This information is often referred to as evidence for simple left-lateral slip on a WNW trending plane [e.g., Shedlock et al., 1985; Wu et al., 1976]. We reexamined the data presented by Wu et al. [1976] and found the measurements difficult to interpret. There are only four trilateration points in the immediate vicinity of the epicentral area, one in each quadrant of the fault plane solution. The observed shortening of 0.38 m between the two stations just to the north of the WNW trending nodal plane is grossly inconsistent with left-lateral slip along the plane. On the other hand, the data cannot be explained by simple right-lateral slip on the other nodal plane either.

It appears that either the deformation (seismic and aseismic) in the epicentral area of this sequence over the 17-year period is quite complex, or that there are internal inconsistencies in the trilateration data. These possibilities are evident from the large amount of shortening (0.20 m) reported for two stations just to the north of the inferred fault with respect to a station ~35 km farther to the north [Wu et al., 1976, Figure 15].

Cipar [1979] synthesized the P and SH waves by using a simple trapezoid source time function with an average duration of about 7 s. He further inferred a bilateral rupture propagation along a WNW trending plane based on the apparent variation in the observed duration of the signals. The waveforms of P waves in the northeastern quadrant of the focal sphere, which

Fig. 3a. (Opposite) Result of the inversion of teleseismic P waves for the Bohai Gulf event of July 18, 1969. The observed seismograms are shown as solid traces along with the synthetics (dashed traces) generated from the best fitting source model (Table 2) composed of two point sources (subevents). Vertical bars on the seismograms indicate the time window used in the inversion. Lower hemisphere, equal area projection of the nodal planes (solid curves for the first subevent, dashed curves for the second) and locations of stations used are shown in the center of the figure. Each subevent is constrained to be a double-couple. The inferred source time function is shown at the bottom of the figure. The rupture propagation during the first subevent is toward the NNE.

TABLE 2. Source Parameters of the Bohai Gulf Event Determined by Inversion of P Waves

Strike, degrees	Dip, degrees	Rake, degrees	Depth, km	Moment, 10^{19} Nm	Time Delay, s	Distance, km	Azimuth, degrees
			Subevent 1				
209±6	87±3	200±17	6±5	4.0±0.2	-	-	-
			Subevent 2				
356±19	80±11	183±8	9±8	2.1±0.3	19±1	14±11	59±38

1. Distance and azimuth are relative to the epicenter, and time delay to the origin time.
2. Realistic estimates of the true uncertainties for focal depth, strike, dip, and rake are shown as ±10σ of the formal uncertainties. Estimates of the uncertainties for the other parameters are shown as ±2 σ of the formal uncertainties [Nábelek, 1984].

were not analyzed by Cipar [1979], are complex. Figure 5 compares the P wave for this event recorded at stations COL and VAL. The signal at VAL appears to be very simple [Cipar, 1979], but signals of significant amplitude are observed for the first minute of the P wave train at COL and other North American stations. These signals appear to be as complicated as those for the Tangshan main shock [Nábelek et al., 1987]. These complicated P waveforms suggest that the deformation associated with the event is quite complex.

Since the distribution of aftershocks suggests left-lateral slip on WNW planes [Shedlock et al., 1985], we have assumed the solution given by Cipar [1979] in the following discussion. Because of its relatively small seismic moment the details of faulting for this event alone do not alter the regional strain significantly.

REGIONAL DEFORMATION DUE TO SEISMIC SLIP

We estimated the deformation due to seismic slip of all events whose seismic moment is greater than or equal to 2.4×10^{17} Nm in the basin since 1946. A similar calculation has been previously carried out by Molnar and Deng [1984], who assumed left-lateral slip for the Bohai Gulf event, and consequently, their conclusion is quite different from ours.

Assuming that a region consists of discrete rigid blocks bounded by faults and that the faults are stationary with respect to a reference block, the average regional deformation ($e_{ij} = \partial u_i/\partial x_j$), including both (irrotational) strain and rigid body rotation, due to earthquake faulting can be estimated from a summation of the asymmetric seismic moment tensor M^*_{ij} of each earthquake [Jackson and McKenzie, 1988; Molnar, 1983]:

$$e_{ij} = (\Sigma M^*_{ij}) / \mu V \qquad i, j = 1, 2, 3 \qquad (1)$$

where μ = rigidity, V = volume of the entire seismogenic region. The asymmetric moment tensor of a double-couple source is defined by

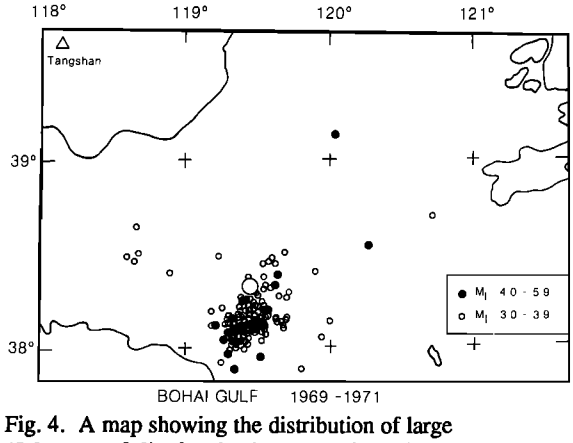

Fig. 4. A map showing the distribution of large ($5.9 > M_l > 3.0$) aftershocks up to 1971 of the Bohai Gulf event of 1969 (redrawn from Figures 6a to 6d of Wei et al. [1984]). The aftershocks form a band trending north-northeast and suggest that the fault plane strikes in that direction.

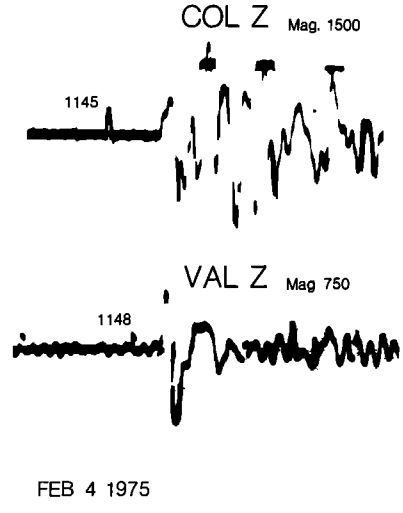

Fig. 5. A comparison of the vertical component, long-period seismogram of the WWSSN for the 1975 Haicheng earthquake recorded at COL, which is located to the northeast of the epicenter, with that recorded at VAL to the northwest. The P waves at COL and other North American stations are complex, lasting at least 60 s. The waveforms suggest a complicated rupture process for this event.

$$M^*_{ij} = M_o b_i n_j \quad (2)$$

where b_i are the components of the unit slip vector, n_i are the components of the unit outward normal of the fault plane, and M_o is the scalar seismic moment [Molnar, 1983].

An interpretation of each element of the asymmetric moment tensor in terms of faulting is displayed graphically in Figure 6. Notice that rigid body rotation $\omega_{ij} = (1/2)(e_{ij} - e_{ji})$. As pointed out by Jackson and McKenzie [1988], this rotation is measured relative to a frame of reference which is attached to the faults. In the simple case of a through-going fault separating two blocks (Figure 6), if the fault remains stationary with respect to one of the blocks, then ω_{ij} represents rotation between the blocks.

There is a set of companion expressions for the symmetric moment tensor M_{ij} [Gilbert, 1970]:

$$M_{ij} = M_o (b_i n_j + b_j n_i) \quad (3)$$

The average (irrotational) strain ε_{ij} in a region is related to the sum of the symmetric moment tensor of individual earthquakes [Kostrov, 1974]:

$$\varepsilon_{ij} = \Sigma M_{ij} / 2\mu V \quad (4)$$

where $\varepsilon_{ij} = (1/2)(e_{ij} + e_{ji})$.

In the case of the North China basin (Figure 1) and during the Tangshan sequence (Figure 2), NNE trending faults appear to be the dominant structure which intersects the boundary of the region of interest. Given the short time window involved, these faults are considered stationary with respect to either of the two blocks to the northwest or southeast of the basin. Therefore the asymmetric moment tensor is a meaningful formulation to detect simple shear across the NNE trending faults in the north China basin.

The North China Basin

The expressions below are the sum of the asymmetric moment tensors (in Nm) and the average regional strain for 16 events (13 individual shocks and their subevents) in the North China basin since 1946 (Table 1):

$$\Sigma M^* = \begin{bmatrix} -0.65 & +0.24 & -0.04 \\ -1.32 & +0.68 & +0.38 \\ -0.07 & -0.27 & -0.03 \end{bmatrix} \times 10^{20} \quad (5a)$$

$$[e_{ij}] = \begin{bmatrix} -1.0 & +0.4 & -0.1 \\ -2.0 & +1.0 & +0.6 \\ -0.1 & -0.4 & -0.0 \end{bmatrix} \times 10^{-7} \quad (5b)$$

given a rigidity of ~3.3×10^{10} N/m^2, an area of 1100 x 900 km^2, and the maximum depth of faulting of ~20 km [Nábelek et al., 1987] for this region. The values shown in (5) are largely determined by the nine shocks with $M_0 \geq 1.4 \times 10^{18}$ Nm ($6.2 \leq M_s \leq 7.8$). The four smallest shocks (17–19, and 22) contributed less than 1% (< 1×10^{18} Nm) of the total scalar seismic moment in (5).

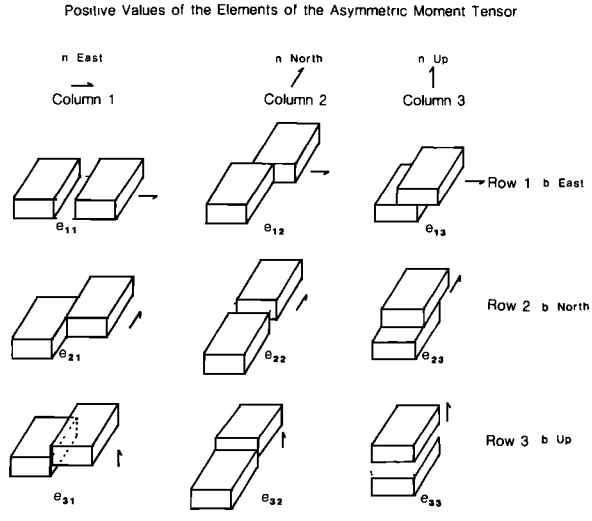

Fig. 6. A schematic diagram showing the geometry of deformation (assumed to be due to a single fault) associated with the positive values of each element of the asymmetric seismic moment tensor of Molnar [1983].

The two events in 1945 and 1967 (M = 6.3) presumably have moments less than 10^{18} Nm and their effects are negligible. Thus the only large event since 1888 which is not accounted for here is the event in 1937 (M = 7). Depending on the frequency-magnitude relationship and magnitude-moment formula, the cumulative seismic slip from small earthquakes below magnitude 6.2 could be as large as that in (5) [Chen and Molnar, 1977]. Therefore we consider (5) as being representative of the pattern of strain due to seismic slip in the North China basin for the past 80–100 years, but the numerical values are lower bounds only.

In map view the dominant component of deformation represented by (5) is right-lateral slip (dextral simple shear strain) along the NNE direction, for the size of e_{21} is about twice as large as either e_{11} or e_{22}, whose positive values represent east-west and north-south extension, respectively. A positive e_{12} is equivalent to right-lateral slip on an east-west trending plane. However, in reality, the small positive value of e_{12} results from the observation that the fault planes of the largest subevents of strike-slip mechanism during the Tangshan main shock trend NNE to NE, instead of exactly north-south.

The rate of seismic slip along NNE trending planes is about 2 to 3 mm/yr when averaged over the past 100 years. The amount of net rotation (or simple shear) is critically dependent on the identification of which nodal plane is the true fault plane. If equal amount of seismic moment was released by right-lateral and left-lateral slip on conjugate nodal planes, the rotation would exactly cancel. The result in (5) reflects the observation that only the Haicheng earthquake of 1975 contributed a significant amount of left-lateral displacement. In contrast, by assuming left-lateral slip for the Bohai event, Molnar and Deng [1984] obtained a dominant pattern of approximately equal amount of north-south extension (e_{22}) and east-west compression (- e_{11}):

$$[e_{ij}] = \begin{bmatrix} -1.8 & -1.0 & +0.4 \\ -1.0 & +2.2 & -0.7 \\ +0.4 & +0.1 & -0.4 \end{bmatrix} \times 10^{-7} \quad (6)$$

Experimenting with different combinations of the data in Table 1 shows that our results for horizontal deformation are practically independent of the choice of fault planes for the dip-slip events because very little strike-slip displacement is associated with them. On the other hand, the relative motion between the top and bottom of the seismogenic zone (e_{i3} and e_{3j}), which occupies approximately the upper two-thirds of the crust, is largely controlled by the orientation of the dip-slip fault planes. Because so few large dip-slip events are observed, crustal thinning ($- e_{33}$) due to seismic slip is small when averaged over the entire region, despite that crustal stretching could be significant locally on small scales.

The Tangshan Sequence

We have also calculated the sum of M^*_{ij} (in Nm) for the Tangshan sequence alone (a total of eight events/subevents):

$$\Sigma M^* = \begin{bmatrix} -0.32 & +0.34 & +0.02 \\ -0.60 & +0.31 & +0.42 \\ -0.12 & -0.13 & +0.01 \end{bmatrix} \times 10^{20} \quad (7)$$

This sequence contributed about 50% of the total slip in expression (5). Nearly the same pattern of horizontal deformation is observed for this sequence as that of (5) where almost all large events in the North China basin in the past 100 years are considered. The only difference is that the size of e_{12} is comparable to the amount of east-west shortening and north-south extension in the source region of the Tangshan sequence, a direct consequence of slip on the NE striking fault plane of the second subevent of the Tangshan main shock, which has the highest moment of all the shocks in the sequence.

Since all the fault plane solutions and seismic moments used here are determined from the analysis of waveforms and absolute amplitudes of P and SH waves, the precision of the moments is probably within 20% [Nábelek, 1984]. Considering possible systematic errors due to effects of local structure and attenuation, the trade-off between duration of the source and depth (therefore moment) for shallow events, and uncertainties in source orientations, we estimate that the accuracy of the dominant components of ΣM^*_{ij} in the horizontal plane is better than 50% (see Molnar and Deng [1984] for additional discussion on errors in ΣM^*_{ij}). At any rate, the relative values of e_{11}, e_{12}, e_{21}, and e_{22} are unlikely to be affected by systematic errors, and we conclude that for both the Tangshan sequence and the entire basin the strain due to seismic slip in the past 100 years is predominantly dextral simple shear strain in the NNE direction with some north-south extension and east-west shortening.

STRIKE-SLIP FAULTING AND THE EVOLUTION OF THE NORTH CHINA BASIN

Reviews of the structure and sedimentation of many pull-apart basins [Aydin and Nur, 1982; Mann et al., 1983; Reading, 1980] in different areas of the globe clearly demonstrate that these basins are usually composite in nature and they typically exhibit several levels of structures at smaller length-scales ("infrastructures"). Small-scale pull-apart structures (basins and sometimes horsts within basins) are enclosed in larger structures and these larger basins are part of even larger ones. Based on ratios between the length and width of many pull-apart basins, Aydin and Nur [1982] suggested a mechanism of forming large pull-apart basins by the successive coalescing of smaller basin infrastructures. Given that the most noticeable features of the deformation associated with the Tangshan sequence are those of a pull-apart system and that the patterns of strain due to seismic slip in the past 100 years are similar at small (~100 km) and basin-wide scales, the high level of seismicity implies that pull-apart structures play an important role in the recent development of the North China basin. Moreover, if we extrapolate this mode of deformation into the Quaternary and Tertiary, a variety of seemingly puzzling geological data can be accounted for by viewing the entire North China basin as a large composite pull-apart structure.

The Overall Shape of the Basin

The overall shape of the basin is that of a "lazy Z" (Figure 1), typical for pull-apart basins formed along right-stepping faults [e.g., Mann et al., 1983]. Based solely on the shape of the basin, Burke and Sengör [1986] independently reached the same conclusion as ours. We interpret the northeastern (the Liaohe fault zone) and southwestern arms (the East Taihang and the Cang Xian-Dongning fault systems) of the North China basin to be analogous to the two master faults in a simple pull-apart basin (Figure 1).

In the case of the North China basin, a single strand of master faults is replaced by a system of faults over a zone of up to about 100 km wide. Large earthquakes occur on both sides of each arm, as well as in the interior of the step between the master fault zones. Because the mechanism of faulting is unknown for the events in 1830 and 1937 (Figure 1), we have no direct information concerning the present-day sense of motion on the master fault systems. We do note, however, that a general right-lateral fault system trending in the NNE direction through the present position of the North China basin has often been invoked both in the reconstruction of the geologic history of eastern China [e.g., Burke and Sengör, 1986; Lu et al., 1983] and in the interpretation of paleomagnetic data [e.g., Courtillot and Besse, 1986; Lee et al., 1987]. Hence the model proposed here is generally consistent with the known large-scale geologic history in the vicinity of the basin.

Quaternary to Recent Development of the North China Basin

Ye et al. [1985] noted that the depocenters of the rapidly accumulating Quaternary sediments approximately coincide with the sites of high surface heat flow (up to 100 mW/m^2). We notice that the depocenters are not interconnected and that low heat flow values can occur next to high heat flow values (Figure 1). These observations, together with the dominant role of strike-slip earthquake faulting and localized regions of

rapid subsidence and transpression, suggest that the pattern of Quaternary tectonic activity in the North China basin can be explained by the cumulative effect of several scales of pull-apart structures resulting from right-lateral slip on a system of right-stepping faults trending NNE to NE.

On one scale we observed this process during the Tangshan sequence. There the maximum amount of subsidence determined from releveling in the small pull-apart regions near Ninghe and Launxian is about 1–1.5 m (Figure 2; Zhang et al. [1981]). These values are comparable to the maximum horizontal slip (2.3 m) observed along the surface rupture of the main shock [Guo et al., 1977]. Therefore the effect of crustal thinning and subsidence can be intensive on small scales (a length on the order of 10 km), but the dominant regional pattern of deformation is strike-slip.

An analogous situation is observed in the Salton Trough, a pull-apart basin resulting from strike-slip motion along the San Andreas fault system, where within the outline of the system of pull-aparts, heat flow values greater than 150 mW/m^2 are observed only 50 km or less from "normal" values (~50 mW/m^2) and extremely high values (> 200 mW/m^2) are measured less than 10 km from those between 80 and 100 mW/m^2. The thickness of sediments is also highly variable on the scale of the length of individual fault segments, but the averaged values of the rate of sedimentation and heat flow over the entire trough and regions immediately surrounding it are not very different from southern California as a whole [e.g., Lachenbruch et al., 1985].

Faulting and the Development of the North China Basin During the Tertiary

Horizontal versus vertical motion. The predominance of dextral simple shear along NNE to NE over vertical motion in and around the North China basin seems to have begun no later than the late Tertiary. Ding and Lu [1983] estimated about 0.1–0.2 mm/yr of relative uplift/subsidence since the mid-Pliocene (about 3.4 Ma ago) from a combination of field and borehole observations including magnetostratigraphy, the position of peneplains, and that of river terraces. Meanwhile, they reported that offsets in drainage patterns indicate horizontal dextral simple shear whose rate is about 2–10 times larger than that of vertical motion. Regardless of the exact origin of the North China basin, dextral simple shear apparently has been the dominant mode of deformation which began no later than the mid-Pliocene and continues today.

Amount of regional crustal thinning and initial subsidence. Assuming a uniform crustal thickness of about 40 km before the initiation of rifting in the Eocene, Hellinger et al. [1985] estimated a total extension of about 30% of the initial length in the basin. This value is larger than that (~20%) obtained from summing the displacement on faults based on reflection surveys [Li, 1982]. However, based on models of regional crustal extension, even 30% of total extension is too small to explain the observed high heat flow values of up to and greater than 100 mW/m^2 [Hellinger et al., 1985]. On the other hand, 20–30% of crustal thinning predicts a total subsidence which is too large for the North China basin in the Paleogene [Hellinger et al., 1985]. This dilemma can be resolved if one accepts the view that the North China basin has evolved as a large composite pull-apart basin driven by motion on strike-slip fault systems rather than the result of regional crustal extension and thinning. In a pull-apart regime the regions of intensive extension occur only at steps of strike-slip faults, and the total amount of crustal thinning on a regional scale resulting from the cumulative effect of localized subsidence over geologic time is much smaller than the maximum values of extension at local pull-aparts.

Variable rates of subsidence in space and time. In a composite pull-apart basin the rate of subsidence and sedimentation is strongly controlled by the spatial configuration of the various scales of strike-slip fault systems within the basin, as well as the history of their displacement, including the occurrence of occasional large earthquakes. One can envision that at different pull-apart sites, rapid crustal thinning and consequently local isostatic compensation have taken place throughout the history of the basin. At the same time, long-term thermal subsidence of each individual pull-apart is complicated by lateral heat transport and continued displacement along strike-slip fault segments [e.g., Sawyer et al., 1987].

Consequently, while the mechanism of basin formation by regional crustal extension and thermal subsidence calls for gradual changes in the rate of subsidence and heat flow over time and space on a basin-wide scale, a composite pull-apart is characterized by continuing fault activity and by rates of subsidence and sedimentation which vary from site to site and fluctuate in time at a given location through most of the history of basin evolution. Indeed, Hellinger et al. [1985] reported that in the North China basin, faulting was evident during the Neogene and that the rate of subsidence not only fluctuated at different times (Paleogene, Neogene, and Quaternary), but also varied from site to site. Similarly, in the Los Angeles basin, which may have a pull-apart origin, Sawyer et al. [1987] successfully modeled the fluctuating rates of subsidence in space and time by dividing the whole basin into several regions of localized extension. The amount of extension within each region varies from 20% up to 178%, while the total extension of the entire basin is only about 66%.

Due to the lack of data, we do not have a detailed map of fault geometry and sedimentary sections to document exactly where the individual pull-apart or push-up structures have developed in the past. We can only speculate that episodes of uplift which apparently occurred during the Neogene in the part of the basin where data are available to Hellinger et al. [1985] could be a result of local transpression. However, if the basin as a whole was uplifted in the same time, such episode would remain unexplained by any of the tectonic models put forward so far, including the one proposed here.

Ye et al. [1985] summarized the pattern of rifting and the distribution of horsts and grabens in the North China basin based on the data published by Li [1981]. At least one clear basin structure which in map view has a similar geometry to that of the present basin can be identified in the Oligocene. That structure is highlighted in Figure 7. This feature is almost entirely a structural low with only a few scattered horsts in it. Even in the Eocene when the basin just began to form, a somewhat smaller structure apparently existed. Again, its geometry is very similar to the present shape of the basin

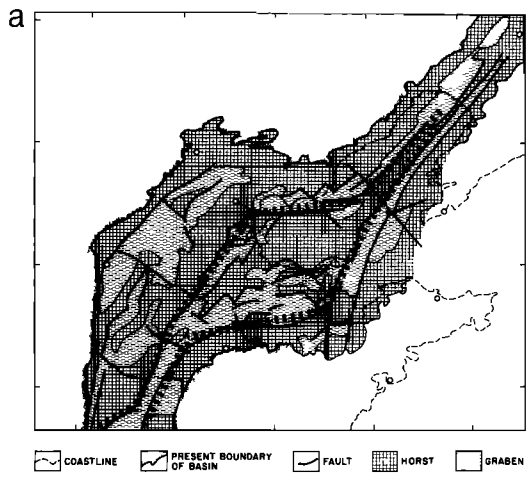

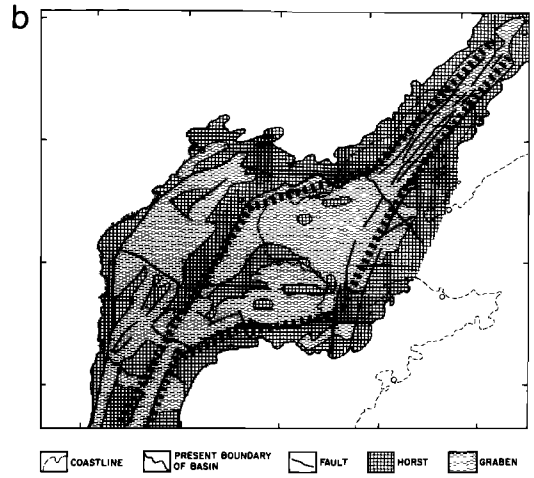

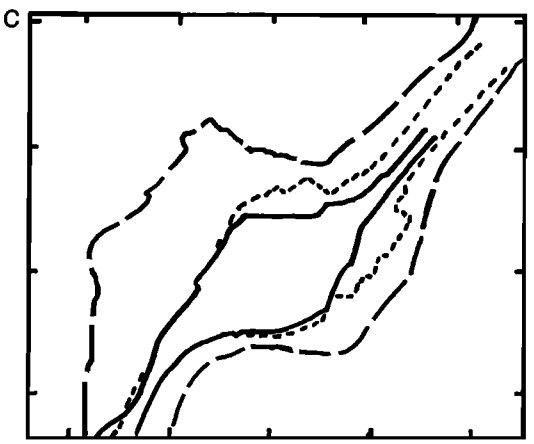

although the structure was in the form of horsts in a larger basin (Figure 7). In both cases, many smaller structures existed elsewhere within the limit of the present basin as well as within the structure that we have outlined in Figure 7. The report by Li [1981] is not detailed enough for us to investigate the geometry of these small structures. The similar geometry ("lazy Z") of structures within the North China basin at the Eocene, Oligocene, and the present, however, suggests that pull-apart structure played an important role in the formation and development of this large sedimentary basin.

DISCUSSION

Active Deformation of Composite Pull-Aparts

Given that smaller pull-aparts can combine to form large composite basins [e.g., Aydin and Nur, 1982; Mann et al., 1983, Reading, 1980], how do small structures evolve while the basin as a whole continues to deform?

The high level of seismic activity in the North China basin provides an unique data set for the pattern of active deformation within a basin at two length scales. The resemblance of the pattern of strain due to recent seismic slip between the Tangshan sequence (length~100 km) and that of the entire basin (~1000 km) indicates that at least some of the infrastructures deform in a manner which is geometrically similar to that of the whole basin. If the deformation associated with other large earthquake sequences is similar to that of the Tangshan sequence, the scattered nature of the seismicity would suggest that the present-day configuration of the basin involves the formation of many smaller pull-apart structures of various scales throughout the basin. Presumably, the interaction of faults on which small earthquakes occur produces only small, localized subsidence, while that of major faults on which large earthquakes take place results in sizable regions of subsidence. The pull-apart regions caused by large faults can overprint the smaller ones, producing subsidence on a regional scale [Nábelek et al., 1987].

It is worth noting that during the Tangshan sequence, there was considerable scatter in the distribution of aftershocks (Figure 2) which cannot be accounted for by uncertainties in the location of the epicenters alone. By combining these locations with the fault plane solutions [Shedlock et al., 1987], some small (< 10 km) pull-apart structures could be

Fig. 7. (Opposite) A map view of two large, basinlike structures with an overall shape of a "lazy Z" within the present boundary of the North China basin which existed during its evolution at different geological times. (a) Map showing the pattern of rifting and graben development during the Eocene [Ye et al., 1985, Figure 8a], based on Li [1981]. The identified large pull-apart structure is outlined by heavy dashed lines. (b) The same as in Figure 7a but during the Oligocene [Ye et al., 1985, Figure 8b]. The identified structure is nearly all filled with sediments. (c) A comparison of the two pull-apart structures identified in Figure 7a (solid curve) and Figure 7b (dashed curve) with the present shape of the basin (broken lines). The geometry of the outline of the basin during the Eocene, Oligocene, and the present time is similar. Several smaller structures whose geometry is not known in detail existed within the ones outlined here.

identified [Nábelek et al., 1987]. Structures like these may be induced or reactivated by the large events. Certainly not all small structures are eliminated by deformation on a larger scale. Thus the mechanism of coalescing infrastructures to form composite basins must be a dynamic process such that while the basin as a whole is growing in size, the infrastructures remain active with new structures being created. Yet, complex structures of various length scales in a composite pull-apart basin are a result of a single driving mechanism: that of motion on the master strike-slip fault system at the sides of the basin.

Dip-Slip Faulting in the North China Basin

Although detailed seismic sections of the North China basin are not available in the open literature, geologic interpretations of reflection profiles often indicate dip-slip faulting [e.g., Hellinger et al., 1985; Li, 1981, 1982; Tang, 1982]. Reflection profiles generally can detect vertical offsets well and there is little doubt that dip-slip motion is present in the North China basin. The published interpretations of reflection profiles are not inconsistent with a pull-apart model of the basin because dip-slip motion is expected within a composite pull-apart basin and because detection of strike-slip faults and the amount of movement associated with them is difficult. Furthermore, the assumption of predominant dip-slip motion after mid-Pliocene conflicts field and borehole observations [Ding and Lu, 1983].

We suggest that secondary structures associated with strike-slip faulting should be searched for in reflection records. For example, local transpression may be common. It may reveal itself as secondary thrust faults and local folding at the intersection of faults, or as the so-called "flower structures." "(Positive) flower structures" are upthrown antiforms (or synforms for "negative flower structures") of sediments bounded by strike-slip faults [e.g., Harding et al., 1983]. The uplift of these sediments is generally accepted to be a result of local transpression [e.g., Sanderson and Marchini, 1984]. We suspect that some of them might originate in pull-apart regions at steps of strike-slip faults where the rapidly depositing sediments are later rotated and squeezed up by continued slip on strike-slip faults.

Other Fault Systems Near the Basin

The overall outline of the North China basin is somewhat complicated by the presence of the nearly north-south trending East Taihang fault on the western border of the southwestern arm (Figure 1). At the present there is no evidence of seismicity related to this fault or any other north-south trending faults within the basin, as seismicity indicates that the NNE trending faults are the dominant active fault system in the interior of the basin.

Outside of the basin, on its southeast side, is the NNE trending Tan-Lu fault zone (Figure 1; Li [1981, Figure 9]). This zone appears to be a major fault system within the North China craton since the Cretaceous [e.g., Lu et al., 1983, Xu et al., 1982]. The zone contains a small amount of Cenozoic sediment in-fill [Li, 1981]. Field mapping in the middle and southern part of this system (southward from the bottom of Figure 1) suggests an early phase of left-lateral motion which changed to right-lateral motion with a component of reverse faulting in the late Tertiary [Lu et al., 1983, Xu et al., 1982]. A very large (M~8.5) earthquake occurred along the trace of this fault system near 35.3°N in 1668 [Seismological Committee of the Academia Sinica, 1956]. Although the present-day rate of motion along the Tan-Lu fault system is poorly known, offsets in the drainage pattern indicate recent right-lateral motion [Ding, 1984].

In the case that the Tan-Lu fault zone has been concurrently active with the two arms of the North China basin and the rate of slip has been approximately equal, then calculations based on the Mohr-Coulomb fracture criterion [e.g., Nur et al., 1986] predict considerable anticlockwise block rotation within the zone between the southern arm of the North China basin and the Tan-Lu fault system. A combination of paleomagnetic data with a detailed search for accommodating strike-slip faults intersecting at 40°–45° with each other in this region may provide important information about the interaction between these two fault systems. In any case, the possibility of continued activity along the Tan-Lu fault presents no conflict to a pull-apart origin of the North China basin as long as movement along the Tan-Lu system is right-lateral [e.g., Lu et al., 1983, Xu et al., 1982].

It is important to note that our model implies that since the mid-Tertiary the southern arm of the North China basin has been a major right-lateral strike-slip system west of the Tan-Lu fault zone which has been frequently assumed to be the only trajectory of major horizontal crustal motion in the North China craton since the Mesozoic [cf., Courtillot and Besse, 1986; Lee et al., 1987].

CONCLUSIONS

The unusually high level of seismicity in the actively subsiding North China basin is largely associated with strike-slip faulting. We analyzed faulting associated with the Tangshan earthquake sequence of 1976 by combining source parameters determined from teleseismic P and SH waves with the location of the largest aftershocks [Nábelek et al., 1987], the distribution of small aftershocks [Shedlock et al., 1987], background seismicity, field observations, and geodetic data to delineate the relationship between strike-slip faulting and subsidence. We conclude that regions of normal faulting and subsidence occur at right-stepping segments of right-lateral strike-slip faults while subsidiary thrust faulting indicates local transpression. Based on the directivity of teleseismic P waveforms and the distribution of aftershocks, we conclude that the Bohai Gulf event of 1969 was also associated with predominantly right-lateral strike-slip motion.

A summation of the asymmetric moment tensors for the largest events in the basin since 1900 shows that the regional strain due to seismic slip is primarily dextral simple shear in the NNE direction. The localized rapid deposition of Quaternary sediments and variable values of high and low heat flow [Ye et al., 1985] can be explained as a result of pulling-apart due to strike-slip motion on numerous faults of different scales in the interior and on the edges of the basin striking subparallel to the two arms of the basin.

This process of basin evolution can be extrapolated back to

the Tertiary by combining the following observations: (1) the overall shape of the basin (a "lazy Z"), which is typical of pull-apart basins formed by right-lateral slipping master faults; (2) horizontal dextral simple shear has dominated over vertical motion since the mid-Pliocene [Ding and Lu, 1983]; (3) the amount of initial subsidence due to faulting was small and the total amount of regional crustal thinning is insufficient to account for the high heat flow values observed at the present [Hellinger et al., 1985]; (4) the rate of subsidence at different locations has varied notably with time since the Eocene and the rate has fluctuated from site to site [Hellinger et al., 1985]; and (5) basinlike structures which are geometrically similar to the present shape of the basin can also be identified in the Oligocene and Eocene (Figure 7).

Acknowledgments. We thank K. Shedlock and Gouyu Ding for helpful discussions. We also thank N. L. Grimison and S. Marshak for critically reading the manuscript. R. V. Sharp and C. Nicholson provided many helpful comments on an earlier draft of the manuscript. This research was supported by NSF grants EAR86-07128 and EAR86-18453.

REFERENCES

Aydin, A., and A. Nur, Evolution of pull-apart basins and their scale independence, *Tectonics*, *1*, 91–105, 1982.

Burke, K., and C. Sengör, Tectonic escape in the evolution of the continental crust, in *Reflection Seismology: The Continental Crust, Geodyn. Ser.*, vol. 14, edited by M. Barazangi and L. Brown, pp. 41–53, AGU, Washington, D. C., 1986.

Butler, R., G. S. Stewart, and H. Kanamori, The July 27, 1976 Tangshan, China earthquake--A complex sequence of intraplate events, *Bull. Seismol. Soc. Am.*, *69*, 207–220, 1979.

Chen, W.-P., and P. Molnar, Seismic moments of major earthquakes and the average rate of slip in central Asia, *J. Geophys. Res.*, *82*, 2945–2969, 1977.

Chung, W. Y., and J. J. Cipar, Source modeling of the Hsingtai, China earthquake of March 1966, *Phys. Earth Planet. Inter.*, *33*, 111–125, 1983.

Cipar, J., Source processes of the Haicheng, China, earthquake from observations of P and S waves, *Bull. Seismol. Soc. Am.*, *69*, 1903–1916, 1979.

Courtillot, V., and J. Besse, Mesozoic and Cenozoic evolution of the North and South China blocks, *Nature*, *320*, 86–87, 1986.

Crowell, J. C., Origin of the late Cenozoic basins in southern California, in *Modern and Ancient Geosynclinal Sedimentation, SEPM Spec. Pub. 19*, edited by R. H. Dott and R. H. Shaver, pp. 292–303, Tulsa, Okla., 1974.

Ding, G., Active faults in China, in *A Collection of Papers of International Symposium on Continental Seismicity and Earthquake Prediction (ISCSEP)*, edited by the Organizing Committee of ISCSEP, pp. 225–242, Seismological Press, Beijing, 1984.

Ding, G., and Y. Lu, On the characteristics of neotectonic deformation of the North China block (in Chinese), *N. China Earthquake Sci.*, *1(2)*, 1–9, 1983.

Dziewonski, A. M., J. E. Franzen, and J. H. Woodhouse, Centroid-moment tensor solutions for October-December, 1983, *Phys. Earth Planet. Inter.*, *34*, 129–136, 1984.

Freund, R., The Hope Fault: A strike-slip fault in New Zealand, *N. Z. Geol. Surv. Bull.*, *86*, 1–49, 1971.

Gilbert, F., Excitation of the normal modes of the Earth by earthquake sources, *Geophys. J. R. Astron. Soc.*, *22*, 223–226, 1970.

Guo, S., Z. Li, S. Chen, X. Chen, X. Chen, Z. Yang, and R. Li, Discussion of the regional structural background and the seismogenic model of the Tangshan earthquake (in Chinese), *Sci. Geol. Sin.*, *4*, 305–321, 1977.

Harding, T. P., R. F. Gregory, and L. H. Stephens, Convergent wrench fault and positive flower structures, Ardmore basin, Oklahoma, in *Seismic Expression of Structural Styles*, vol. 3, *Stud. Geol. Ser.*, *15*, edited by A. W. Balley, pp. 4.2-13–4.2-17, AAPG, Tulsa, Okla., 1983.

Harland, W. B., Tectonic transpression in Caledonian Spitsbergen, *Geol. Mag.*, *108*, 27–42, 1971.

Hellinger, S. J., and J. G. Sclater, Some comments on two-layer extensional models for the evolution of sedimentary basins, *J. Geophys. Res.*, *88*, 8251–8269, 1983.

Hellinger, S. J., K. M. Shedlock, J. G. Sclater, and H. Ye, The Cenozoic evolution of the North China Basin, *Tectonics*, *4*, 343–358, 1985.

Jackson, J., and D. McKenzie, The relationship between plate motions and seismic moment tensors, and the rates of active deformation in the Mediterranean and Middle East, *Geophys. J. R. Astr. Soc.*, *93*, 45–73, 1988.

Kikuchi, M., and H. Kanamori, Inversion of complex body waves, II, *Phys. Earth Planet. Inter.*, *43*, 205–222, 1986.

Kostrov, V. V., Seismic moment and energy of earthquakes, and seismic flow of rock, *Izv. Acad. Sci. USSR, Phys. Solid Earth, Engl. Transl.*, *1*, 23–44, 1974.

Lachenbruch, A. H., J. H. Sass, and S. P. Galanis, Jr., Heat flow in southernmost California and the origin of the Salton Trough, *J. Geophys. Res.*, *90*, 6709–6736, 1985.

Lee, G., J. Besse, and V. Courtillot, Eastern Asia in the Cretaceous: New paleomagnetic data from South Korea and a new look at Chinese and Japanese data, *J. Geophys. Res.*, *92*, 3580–3596, 1987.

Lee, K. Y., Geology of the petroleum and coal deposits in the North China Basin, eastern China, *U. S. Geol. Surv. Open File Rep.*, *86-154*, 57 pp., 1986.

Lee, W. H. K., F. T. Wu, and S. C. Wang, A catalog of instrumentally determined earthquakes in China (magnitude > 6) compiled from various sources, *Bull. Seismol. Soc. Am.*, *68*, 383–398, 1978.

Li, D., Geological structure and hydrocarbon occurrence of the Bohai gulf oil and gas basin (China), in *Petroleum Geology in China*, edited by J. F. Mason, pp. 180–192, PennWell, Tulsa, Okla., 1981.

Li, D., Tectonic frameworks of the Bohai Gulf and coastal basins, *Acta Oceanol. Sinica*, *1*, 82–93, 1982.

Li, Z., and S. Guo, On the relationship between the Ninghe 6.9 aftershock and the Tangshan earthquake from the viewpoint of seismotectonics (in Chinese), *Seismol. Geol.*, *1(4)*, 27–35, 1979.

Lu, H., H. Yu, Y. Ding, and Q. Zhang, Changing stress field

in the middle segment of the Tan-Lu fault zone, eastern China, *Tectonophysics*, *98*, 253–270, 1983.

Mann, P., M. R. Hempton, C. Bradley, and K. Burke, Development of pull-apart basins, *J. Geol.*, *91*, 529–554, 1983.

McKenzie, D., Some remarks on the development of sedimentary basins, *Earth Planet. Sci. Lett.*, *40*, 25–32, 1978.

Molnar, P., Average regional strain due to slip on numerous faults of different orientations, *J. Geophys. Res.*, *88*, 6430–6432, 1983.

Molnar, P., and Q. Deng, Faulting associated with large earthquakes and the average rate of deformation in central and eastern Asia, *J. Geophys. Res.*, *89*, 6203–6227, 1984.

Nábelek, J. L., Determination of earthquake source parameters from inversion of body waves, Ph.D. thesis, Mass. Inst. of Technol., Cambridge, 1984.

Nábelek, J., W.-P. Chen, and H. Ye, The Tangshan earthquake sequence of 1976 and its implications for the evolution of the North China basin, *J. Geophys. Res.*, *92*, 12,615–12,628, 1987.

Nur, A., H. Ron, and O. Scotti, Fault mechanics and the kinematics of block rotations, *Geology*, *14*, 746–749, 1986.

Peng, K., L. Xie, S. Li, D. M. Boore, W. D. Iwan, and T. L. Teng, The near-source strong-motion accelerograms recorded by an experimental array in Tangshan, China, *Phys. Earth Planet. Inter.*, *38*, 92–109, 1985.

Reading, H. G., Characteristics and recognition of strike-slip fault systems, in *Sedimentation in Oblique-Slip Mobile Zones, Int. Assoc. Sedimentol. Spec. Publ.*, *4*, edited by P. F. Ballance and H. G. Reading, pp. 7–26, Liege, Belgium, 1980.

Sanderson, D. J., and W. K. Marchini, Transpression, *J. Struct. Geol.*, *6*, 449–458, 1984.

Sawyer, D. S., A. T. Hsui, and M. N. Toksöz, Extension, subsidence and thermal evolution of the Los Angeles basin--A two dimensional model, *Tectonophysics*, *133*, 15–32, 1987.

Segall, P., and D. D. Pollard, Mechanics of discontinuous faults, *J. Geophys. Res.*, *85*, 4337–4350, 1980.

Seismological Committee of the Academia Sinica, *Chronological Tables of Earthquake Data of China* (in Chinese), Science Press, Beijing, 1956.

Sharp, R. V., Tectonic setting of the Salton Trough, *U. S. Geol. Surv. Prof. Pap.*, *787*, 3–15, 1972.

Shedlock, K. M., L. M. Jones, and X. Ma, Determination of elastic wave velocity and relative hypocenter locations using refracted waves, II, Application to the Haicheng, China, aftershock sequence, *Bull. Seismol. Soc. Am.*, *75*, 427–439, 1985.

Shedlock, K. M., J. Baranowski, W.-W. Xiao, and X-L. Hu, The Tangshan aftershock sequence, *J. Geophys. Res.*, *92*, 2791–2803, 1987.

State Seismological Bureau, *Tangshan Earthquake of 1976* (in Chinese), Seismology Publisher, Beijing, 1982.

Tang, Z., Tectonic features of oil and gas basins in eastern part of China, *Am. Assoc. Pet. Geol. Bull.*, *66*, 509–521, 1982.

Tangshan Seismological Team, The Tangshan earthquake sequence (in Chinese), in *Observation and Investigation of Tangshan Earthquake*, pp. 74–80, Seismology Publisher, Beijing, 1981.

Tapponnier, P., and P. Molnar, Slip-line field theory and large scale continental tectonics, *Nature*, *264*, 319–324, 1976.

Tapponnier, P., and P. Molnar, Active faulting and Cenozoic tectonics of China, *J. Geophys. Res.*, *82*, 2905–2930, 1977.

Wei, G., T. Ji, and B. Li, Characteristics of magnitude 7.4 earthquake sequence in the Bohai area (in Chinese), *Seismol. Geol.*, *6*, 21–29, 1984.

Wu, K.-T., M.-S. Yue, H.-Y. Wu, X.-L. Cao, H.-T. Chen, W.-Q. Huang, K.-Y. Tian, and S.-D. Lu, Certain characteristics of Haicheng earthquake (M = 7.3) sequence (in Chinese), *Acta. Geophys. Sin.*, *19*, 95–109, 1976. (*Chin. Geophys., Engl. Transl.*, *1*, 289–308, 1978).

Xiang, H., M. Ding, and F. Song, Analysis of tectonic condition for 1978 Haicheng earthquake with magnitude of 6.0 (in Chinese), *Seismol. Geol.*, *2(2)*, 61–69, 1980.

Xu, Z., Q. Zhang, and M. Zhao, The main characteristics of the paleorift in the middle section of the Tancheng-Lujiang fracture zone (in Chinese with English abstract), *Bull. Chin. Acad. Geol. Sci.*, *4*, 17–40, 1982.

Ye, H., K. M. Shedlock, S. J. Hellinger, and J. G. Sclater, The North China basin: An example of a Cenozoic rifted intraplate basin, *Tectonics*, *4*, 153–169, 1985.

Zhang, Z.-L., Q.-Z. Li, J.-C. Gu, Y.-M. Jin, M.-Y. Yang, and W.-Q. Liu, The fracture processes of the Tangshan earthquake and its mechanical analysis (in Chinese), *Acta Seism. Sinica*, *2(2)*, 111–129, 1980.

Zhang, Z., J. Xie, F. Xu, L. Huang, H. Hu, S. Peng, S. Ying, and S. Gen, Tangshan earthquake and crustal deformation, in *Observation and Investigation of Tangshan Earthquake* (in Chinese), pp. 163–183, Seismology Publisher, Beijing, 1981.

W.-P. Chen, 245 NHB, 1301 W. Green Street, Department of Geology, University of Illinois, Urbana, IL 61801.

J. Nábelek, College of Oceanography, Oregon State University, Corvallis, OR 97331.

(Received May 2, 1986;
revised May 2, 1988;
accepted May 3, 1988.)